Automatic Mirror Alignment for VIRGO: First experimental demonstration of the Anderson technique on a large-scale interferometer.

F. Acernese[‖], P. Amico[x], S. Aoudia[**], N. Arnaud[††], S. Avino[‖], D. Babusci[§], G. Ballardin[†], R. Barillé[†], F. Barone[‖], L. Barsotti[xi], M. Barsuglia[††], F. Beauville[*], M.A. Bizouard[††], C. Boccara[‡‡], F. Bondu[**], L. Bosi[x], C. Bradaschia[xi], S. Braccini[xi], A. Brillet[**], V. Brisson[††], L. Brocco[xii], D. Buskulic[*], G. Calamai[‡], E. Calloni[‖], E. Campagna[‡], F. Cavalier[††], R. Cavalieri[†], G. Cella[xi], E. Chassande-Mottin[**], F. Cleva[**], J.-P. Coulon[**], E. Cuoco[†], V. Dattilo[†], M. Davier[††], R. De Rosa[‖], L. Di Fiore[‖], A. Di Virgilio[xi], B. Dujardin[**], A. Eleuteri[‖], D. Enard[†], I. Ferrante[xi], F. Fidecaro[xi], I. Fiori[xi], R. Flaminio[*], J.-D. Fournier[**], S. Frasca[xii], F. Frasconi[†], A. Freise[†], L. Gammaitoni[x], A. Gennai[xi], A. Giazotto[xi], G. Giordano[§], L. Giordano[‖], R. Gouaty[*], D. Grosjean[*], G. Guidi[‡], S. Hebri[**], H. Heitmann[**], P. Hello[††], P. Heusse[††], L. Holloway[†], S. Kreckelbergh[††], P. La Penna[†], V. Loriette[‡‡], M. Loupias[†], G. Losurdo[‡], J.-M. Mackowski[¶], E. Majorana[xii], C. N. Man[**], F. Marchesoni[x], E. Marchetti[‡], F. Marion[*], J. Marque[†], F. Martelli[‡], A. Masserot[*], M. Mazzoni[‡], L. Milano[‖], C. Moins[†], J. Moreau[‡‡], N. Morgado[¶], B. Mours[*], J. Pacheco[**], A. Pai[xii], C. Palomba[xii], F. Paoletti[†], S. Pardi[‖], A. Pasqualetti[†], R. Passaquieti[xi], D. Passuello[xi], S. Peirani[**], B. Perniola[‡], L. Pinard[¶], R. Poggiani[xi], M. Punturo[x], P. Puppo[xii], K. Qipiani[‖], P. Rapagnani[xii], V. Reita[‡‡], A. Remillieux[¶], F. Ricci[xii], I. Ricciardi[‖], P. Ruggi [†], G. Russo[‖], S. Solimeno[‖], A. Spallicci[**], R. Stanga[‡], R. Taddei[†], D. Tombolato[*], E. Tournefier[*], F. Travasso[x], D. Verkindt[*], F. Vetrano[‡], A. Viceré[‡], J.-Y. Vinet[**], H. Vocca[x], M. Yvert[*] and Z.Zhang[†]

[*]Laboratoire d'Annecy-le-Vieux de Physique des Particules, Annecy-le-Vieux, France;
[†]European Gravitational Observatory (EGO), Cascina (Pi), Italia;
[‡]INFN, Sezione di Firenze/Urbino, Sesto Fiorentino, and/or Università di Firenze, and/or Osservatorio Astrofisico di Arcetri, Firenze and/or Università di Urbino, Italia;
[§]INFN, Laboratori Nazionali di Frascati, Frascati (Rm), Italia;
[¶]SMA, IPNL, Villeurbanne, Lyon, France;
[‖]INFN, sezione di Napoli and/or Università di Napoli "Federico II" Complesso Universitario di Monte S.Angelo, and/or Università di Salerno, Fisciano (Sa), Italia;
[**]Departement Artemis – Observatoire de la Côte d'Azur, BP 42209 06304 Nice, Cedex 4, France;
[††]Laboratoire de l'Accélérateur Linéaire (LAL), IN2P3/CNRS-Univ. de Paris-Sud, Orsay, France;
[‡‡]ESPCI, Paris, France;
[x]INFN, Sezione di Perugia and/or Università di Perugia, Perugia, Italia;
[xi]INFN, Sezione di Pisa and/or Università di Pisa, Pisa, Italia;
[xii]INFN, Sezione di Roma and/or Università "La Sapienza", Roma, Italia.

arXiv:gr-qc/0411116v1 24 Nov 2004

***Abstract*— The French-Italian interferometric gravitational wave detector VIRGO is currently being commissioned. Its principal instrument is a Michelson laser interferometer with 3 km long optical cavities in the arms and a power-recycling mirror. The interferometer resides in an ultra-high vacuum system and the mirrors are suspended from multistage pendulums for seismic isolation.**

This type of laser interferometer reaches its maximum sensitivity only when the optical setup is held actively very accurately at a defined operating point: control systems using the precise interferometer signals stabilise the longitudinal and angular positions of the optical component. This paper gives an overview of the control system for the angular degrees of freedom; we present the current status of the system and report the first experimental demonstration of the Anderson technique on a large-scale interferometer.

***Index Terms*— gravitational wave detector, laser interferometer, automatic alignment, VIRGO**

Send correspondence to A. Freise, E-mail: andreas.freise@ego-gw.it

I. Introduction

THE French-Italian collaboration VIRGO [1] has built a large-scale interferometric gravitational-wave detector near Pisa, Italy. The main instrument is a Michelson interferometer (MI) with 3 km long Fabry-Perot (FP) cavities in its arms. High-quality optics are suspended to act as quasi-free

test masses at the end of the Michelson interferometer arms so that a gravitational wave, passing perpendicular to the detector, will be detected in the interferometer signal. The Fabry-Perot cavities in the arms enhance the light power and thus increase the optical gain of the interferometer. The apparatus is designed to achieve a relative displacement sensitivity of better than $\delta l/l = 10^{-21}/\sqrt{\mathrm{Hz}}$ between 20 Hz and 10 kHz. The sensitivity will be limited by seismic disturbances below 3 Hz, by thermal noise up to 100 Hz and by shot noise for higher frequencies.

In order to reach this extreme sensitivity, the VIRGO detector uses special techniques to minimise the coupling of noise into the interferometric signal. The large optics (mirrors and beam splitters) are super-polished fused silica pieces with very low absorption and scattering. They are located in an ultra-high vacuum system and suspended from a sophisticated seismic isolation system, the so-called superattenuator [2]. The superattenuator consists of a multistage pendulum and offers an enormous passive isolation from seismic motion for Fourier frequencies larger than its mechanical resonance frequencies (10^{14} at 10 Hz). However, the motion at the resonance frequencies (between 10 mHz and 4 Hz) can be large and must be reduced by active control.

The optics of the Michelson interferometer and of the cavities have to be well-aligned with respect to each other and with respect to the incoming beam to reach their high optical qualities. The angular degrees of freedom of the suspended optics show a non-negligible deviations which, if uncontrolled, distort the cavity eigen-modes and also the interference at the beam splitter. This causes power modulation of the light fields; long term drifts will make a longitudinal control impossible after a certain amount time; and furthermore, mis-alignments increase the coupling of other noise sources into the main detector output. To guarantee a stable long-term operation and a high sensitivity the angular degrees of freedom have to be actively controlled.

II. Optical Layout

Figure 1 shows a simplified optical layout of the VIRGO interferometer in the recombined configuration. Although the MI in the recombined configuration does not provide a detector sensitive enough for detecting gravitational waves, it is the final step on the way to the detector with recycling. It allows to characterise the optical signals to implement the proper control system for the recycled interferometer, for example, for the frequency stabilisation or the automatic alignment.

The laser light, 20 W @1064nm provided by an injection-locked master-slave solid state laser (Nd:YAG), enters the vacuum system at the *injection bench* (IB). The beam is spatially filtered by a 144 m long input mode-cleaner cavity (IMC) before being injected into the main interferometer.

The laser frequency is pre-stabilised using the IMC cavity as a reference. The low-frequency stability is achieved by an additional control system that stabilises the IMC length below 15 Hz to the length of a so-called reference cavity (RFC).

A beam with 10 W of power enters the Michelson interferometer through the power-recycling mirror. In the recombined configuration the power-recycling mirror is largely misaligned so that it merely attenuates the beam without interacting with the rest of the interferometer. In consequence, a beam with approximately 800 mW is impinging on the main beam splitter. It is split into two beams that are injected into the 3 km long arm cavities. The finesse of the arm cavities is approximately 50; this yields a circulating light power of 13 W. The flat input mirrors and the spherical end mirrors form a stable resonator with the beam waist being at the input mirrors with a radius of approximately 20 mm.

The MI is held on the dark fringe, and the expected gravitational wave signal will be measured in the beam from the dark port, which is passed through an *output mode cleaner* (OMC), a 2.5 cm long rigid cavity and then detected on photo diode B1 (in fact, B1 is a group of 16 InGaAs photo diodes).

The interferometer control systems utilise the interferometer output signals and a modulation-demodulation method. For this purpose the laser beam is modulated in phase with a electro-optic modulator (EOM, see Figure 1) at $f_{\mathrm{RF}} = 6.26\,\mathrm{MHz}$. Such a phase modulation generates new frequency components with a frequency offset of $\pm f_{\mathrm{RF}}$ to the frequency of the laser beam f_0. These frequency components are called *sidebands*, and the light field at f_0 is called *carrier*

The photo currents detected by the photo diodes in several output ports of the interferometer are then demodulated with the same frequency f_{RF} or multiples of that frequency. The demodulated signals from single element diodes (B1 to B8) are used for the length control of the interferometer, whereas the demodulated signals from split photo detectors (Q21 to Q82) provide control signals for the angular degrees of freedom of the interferometer mirrors.

The modulation-demodulation technique is commonly used in many interferometers, especially in the other interferometric gravitational wave detectors (LIGO, TAMA and GEO 600 [3]–[5]). However, for each interferometer a unique control topology has been developed, depending on the details of the experimental realisation of the optical system [6].

III. Alignment sensing and control

The automatic alignment of the interferometer consists of two types of control: the *linear alignment* measures the mirror positions with respect to the laser beam and feeds back to the mirrors angular positions (bandwidth $\approx$ 5 Hz), and the *drift control*: a low frequency (bandwidth < 100 mHz) control measures the beam axis position in the two interferometer arms and feeds back to the beam splitter and the injection bench angular position.

The specifications given for the alignment control require that the angular fluctuations are reduced to $10^{-7}\,\mathrm{rad_{RMS}}$ for the recycling mirror, $2 \cdot 10^{-8}\,\mathrm{rad_{RMS}}$ for the cavity input mirrors and $3 \cdot 10^{-9}\,\mathrm{rad_{RMS}}$ for the cavity end mirrors.

During the lock acquisition process the mirrors and the beam splitter are controlled by local control systems that keep the mirrors aligned with respect to local references [7]. These controls can reduce the angular fluctuations of the mirrors to

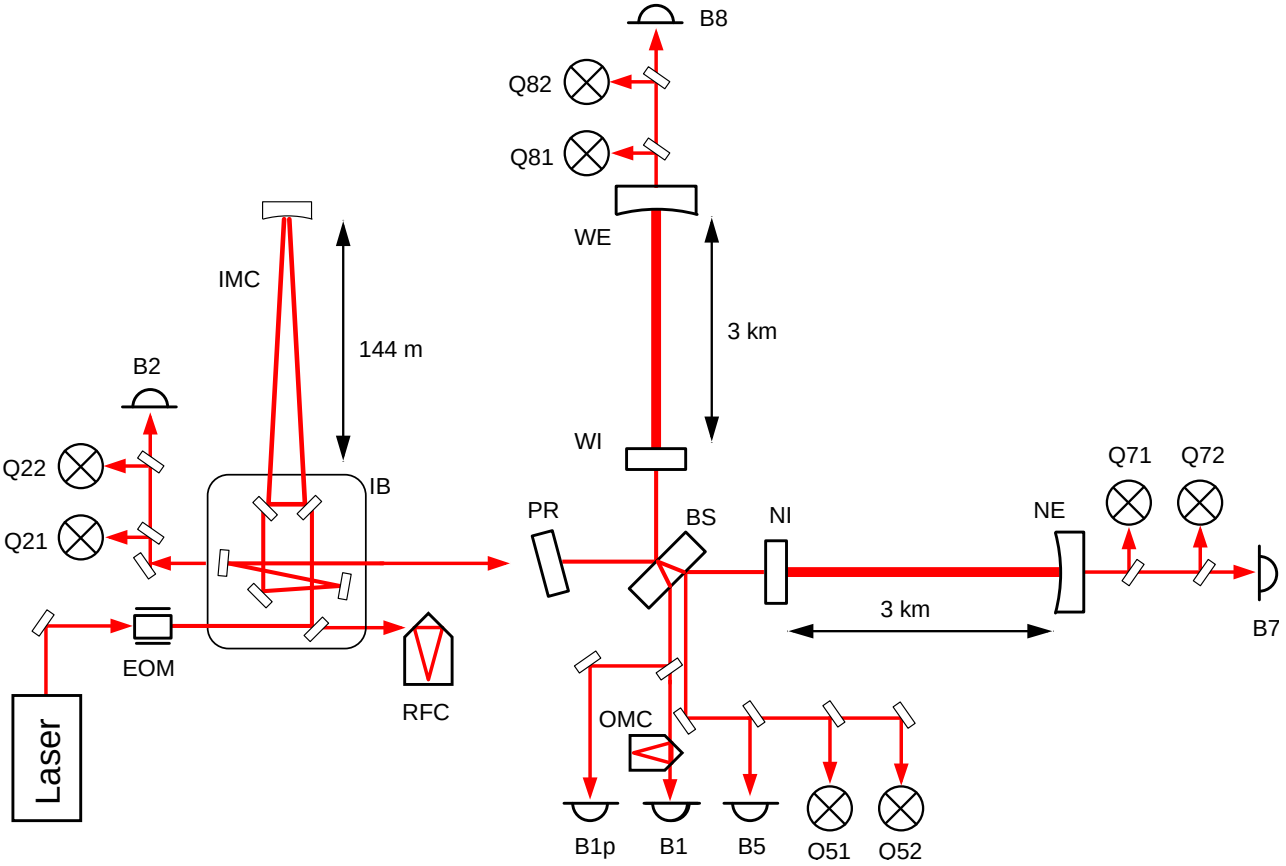

Fig. 1

A SIMPLIFIED SCHEMATIC OF THE OPTICAL DESIGN FOR VIRGO: THE LASER BEAM IS DIRECTED ON THE *detectors table* (DT) INTO THE FIRST VACUUM CHAMBER, THE INJECTION TOWER, IN WHICH ALL OPTICAL COMPONENTS ARE ATTACHED TO A SUSPENDED OPTICAL BENCH, THE *injection bench* (IB). AFTER PASSING THE *input mode cleaner* (IMC), THE BEAM IS INJECTED THROUGH THE *power-recycling mirror* (PR) INTO THE MAIN INTERFEROMETER. THE BEAM IS SPLIT AND ENTERS THE TWO 3 KM LONG ARM CAVITIES, THE *west arm* (WA) AND *north arm* (NA). THE MICHELSON INTERFEROMETER (MI) IS HELD AT THE DARK FRINGE SO THAT MOST OF THE LIGHT POWER IS REFLECTED BACK TO THE *power-recycling mirror* (PR). IN THE FINAL CONFIGURATION THE PR TOGETHER WITH THE MI FORM A FABRY-PEROT-LIKE CAVITY IN WHICH THE LIGHT POWER IS ENHANCED. IN THE RECOMBINED CONFIGURATION THE PR IS LARGELY MISALIGNED AND CAN BE SIMPLY CONSIDERED AS AN ATTENUATOR WITH A TRANSMISSION OF 8%. THE LIGHT FROM THE DARK PORT OF THE BEAM SPLITTER IS FILTERED BY AN *output mode cleaner* (OMC) BEFORE BEING DETECTED ON A SET OF 16 PHOTO DIODES (B1), WHICH GENERATE THE MAIN OUTPUT SIGNAL OF THE DETECTOR. THE OTHER PHOTO DIODES SHOWN IN THIS SCHEMATIC WITH NAMES STARTING WITH **B** ARE USED FOR LONGITUDINAL CONTROL OF THE INTERFEROMETER; DIODES NAMED WITH A **Q** REPRESENT SPLIT PHOTO DETECTORS USED FOR ALIGNMENT CONTROL.

a few microradians RMS over a time period of one hour. But the local control can neither achieve the required long term stability nor the low noise spectral density.

The purpose of the linear alignment is to provide a global control for the mirror alignment that uses the most precise error signals derived from the interferometer itself. Thus, after the interferometer has reached its operating condition, the controls of the angular positions should be switched from the local controls to the linear alignment.

The control topology for the linear alignment of VIRGO has been designed and tested using time domain simulations and a table-top prototype experiment [8].

A. Modulation frequency

The control system for the VIRGO interferometer is unique in two ways: first, only one modulation is used to derive control signals for all longitudinal and angular degrees of freedom of the main interferometer. Second, as the only large-scale interferometer VIRGO makes use of the Anderson technique [9] in the sense that it uses the light transmitted by the arm cavities to generate differential wave-front signals.

This design requires a carefully chosen modulation frequency and carefully tuned cavity lengths. The respective cavities are: the input mode cleaner cavity of $L_{\mathrm{IMC}} \approx 144\,\mathrm{m}$, the arm cavities with $L_{\mathrm{FP}} \approx 3\,\mathrm{km}$ and the short power-recycling cavity

formed by PR with NI and WI with a length of $L_{\mathrm{PRC}} \approx 12.07\,\mathrm{m}$. The sideband frequency and the cavity lengths have to be set following an exact scheme:

- in order to pass the sidebands through the IMC the modulation frequency must be an exact multiple of the IMC's free spectral range: $f_{\mathrm{RF}} = N\ \mathrm{FSR}_{\mathrm{IMC}}$ with N as an integral number. This condition has to be tuned very carefully because a mismatch of only a few Hz couples lengths noise of the IMC into the main interferometer signals.
- for the longitudinal control signals the sidebands should be anti-resonant in the arm cavities and resonant in power-recycling cavity. This can be achieved if the sideband frequency is a) not an exact multiple of the arm cavities free spectral range and b) the sideband frequency is chosen such that $f_{\mathrm{RF}} = \mathrm{FSR}_{\mathrm{PRC}}/2$. An accurate tuning of this condition is desirable to achieve an intrinsic decoupling of the longitudinal control signals but a deviation of a few kHz can be tolerated. Note that in the recombined configuration the power-recycling cavity is not present so that this condition can be ignored.
- the Anderson technique requires the modulation frequency to be a resonance frequency of the TEM_{01} mode in the arm cavities. Thus:

$$f_{\mathrm{RF}} = N\ \mathrm{FSR}_{\mathrm{FP}} + f_{\mathrm{sep}} \tag{1}$$

with N as a integral number, $\mathrm{FSR}_{\mathrm{FP}}$ the free spectral range of the arm cavity and f_{sep} the mode separation frequency, which is the difference between the resonance frequencies of TEM modes for different mode numbers:

$$\begin{aligned} f_{\mathrm{sep}} &= f_{\mathrm{n+1,m}} - f_{\mathrm{n,m}} \\ &= \tfrac{c}{2\pi L_{\mathrm{FP}}} \arccos\left(\sqrt{1 - L_{\mathrm{FP}}/R_C}\right) \end{aligned} \tag{2}$$

with $f_{\mathrm{n,m}}$ being the resonance frequency of a TEM_{nm} mode, c, the speed of light and R_C the radius of curvature of the cavity end mirror.

The modulation frequency must be tuned with respect to this value given by the cavity length and the mirror curvature. The tolerance is $\pm 500\,\mathrm{Hz}$, given by the linewidth of the arm cavities.

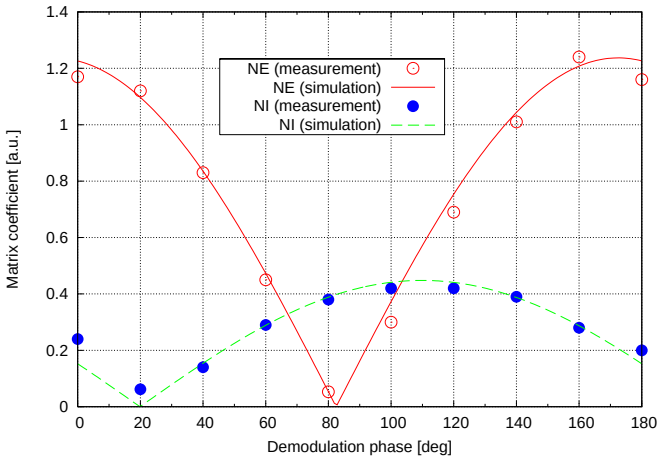

Fig. 2

THIS PLOT SHOWS THE AMPLITUDE OF THE SENSING MATRIX COEFFICIENTS FOR Q71 AS A FUNCTION OF THE ELECTRONIC DEMODULATION PHASE: THE MEASURED DATA WERE OBTAINED WITH THE NORTH ARM CAVITY LONGITUDINALLY CONTROLLED: A SINUSOIDAL DISTURBANCE OF KNOWN AMPLITUDE WAS INJECTED TO THE RESPECTIVE MIRROR AND THE CORRESPONDING AMPLITUDE IN THE QUADRANT SIGNAL MEASURED. THE SIMULATED VALUES WERE PRODUCED BY COMPUTING THE DC VALUE OF THE TRANSFER FUNCTION: MIS-ALIGNMENT ANGLE→ DIFFERENTIAL WAVE FRONT SIGNAL. BY CHOOSING THE CORRECT DEMODULATION PHASE A COMPLETE SIGNAL SEPARATION CAN BE ACHIEVED.

B. Alignment error signals

The sensors for the alignment control are *quadrant split photo detectors* (or *quadrant diodes* for short). These are photo diodes with 4 separate elements, so called quadrants. The quadrants have an active area of $25\,\mathrm{mm}^2$ each and are oriented at $45°$. The four quadrants (up, down, left, right) are separated by a 125 micrometers wide gap and form together a circular photo sensitive area.

Each quadrant diode can provide a multitude of signals: The sum over four quadrants gives the same signal as a normal photo diode. In order to generate alignment control signals the differences between the upper and lower elements and the left and right elements are computed. These signals give the vertical and horizontal positions of the beam on the diode and serve as error signals for the drift control.

A demodulation of a differential quadrant output at f_{RF} yield two additional outputs: the in-phase and quadrature signal contain information about the angle and position (vertical and horizontal respectively) of the phase front of the carrier with respect to the sidebands. These signals can provide very accurate error signal for an automatic alignment system if the optical setup is composed in such a way that a misalignment of a mirror produces a spatial separation between the carrier and the sidebands. This method is called differential wavefront sensing and is used to obtain error signals for the linear alignment control. For a single Fabry-Perot cavity the alignment control signals can be derived in reflection of the cavity (Ward method [10]) or in transmission of the cavity (Anderson method [9]). The automatic alignment system in VIRGO uses also the light transmitted by the arm cavities and can thus be considered as an extension of the Anderson technique: The quadrant diodes are arranged in pairs. Four sets of two quadrants each are located in four of the interferometer outputs (see Figure 1): in reflection (Q21, Q22), at the reflection of the anti-reflex coated surface of the beam splitter (Q51, Q52) and in transmission of the arm cavities (Q71, Q72, Q81, Q82). Adjustable lens telescopes are used so that the beam impinging on the two quadrants of each pair has a Gouy phase difference of $90°$.

C. Sensing Matrix

The linear alignment of the VIRGO interferometer controls ten degrees of freedom: the angular positions of the four arm cavity mirrors (NI, NE, WI and WE) plus the angular position of the PR mirror[1].

In the recombined configuration the two arm cavities are completely decoupled and can be treated as completely separated. In the case of final VIRGO configuration this is not longer the case; all 10 degrees of freedom are strongly coupled.

In general, a demodulated signal of a quadrant detector represents a linear combination of the various angular degrees of freedom of the optical system. In order to design control systems of a complex system like the VIRGO interferometer it is important to reduce the coupling between the various degrees of freedom in the sensors.

In the following we assume that the cavity mirrors and the optical readout have been set up well, so that the horizontal and vertical degrees of freedom can be treated completely separately.

A further separation of the several degrees of freedom in one quadrant diode signal can be achieved by tuning the Gouy phase Ψ. For a simple Fabry-Perot cavity with one plane and one curved mirror one can use one quadrant diode in near field ($\Psi = 0°$) to measure the alignment of the flat mirror and one quadrant in the far field ($\Psi = 90°$) to measure the curved mirror misalignment.

The optimum Gouy phases for the VIRGO interferometer have been computed using a interferometer simulation. Adjustable telescopes are used to set the Gouy phases to these values and to allow a further adjustment to correct for the unavoidable discrepancies between the experimental realisation and the simulation.

Finally the demodulation phase for each quadrant diode can be set in order to minimise the coupling of error signals . When the interferometer is at its operating point the dependence of the quadrant signals on the mirror positions can be described by a static matrix. For example, if we only consider the vertical alignment of north arm cavity mirrors NI and NE the signals on the quadrant diode Q71 and Q72 are given as

$$(Sp_{\mathrm{Q71}}, Sq_{\mathrm{Q71}}, Sp_{\mathrm{Q72}}, Sq_{\mathrm{Q72}}) = \mathbf{M} \cdot (\Theta_{\mathrm{NI}}, \Theta_{\mathrm{NE}}) \quad (3)$$

with Sp representing the in-phase component of the demodulated signal, Sq the quadrature component, Θ_{NI} and Θ_{NE} the misalignment angles of the cavity mirrors and $\mathbf{M}$ the so-called sensing matrix.

The matrix coefficients depend on the demodulation phase and on the Gouy phase of the beam on the detector. Electronic phase shifters allow to control the demodulation phases such that the coupling of the various degrees is reduced. Figure 2 shows the measured and simulated matrix coefficient amplitudes for Q71 as a function of the demodulation phase.

The demodulated signal from all quadrant diodes are acquired as a digital signal, sampled at 500 Hz. A dedicated processor computes the misalignment angles with a linear reconstruction method using the measured sensing matrix. This is part of the *Global Control*, a combination of hardware and software which is used to compute corrections signals from photo diode error signals [11].

The Global Control sends the alignment signals to digital signal processors (DSP) controlling the suspensions [12]. The DSPs apply the necessary control filters to compensate the mechanical transfer function of the suspended mirror and send the correction signals to the actuators of the suspension.

[1]The angular motion of the beam splitter does not represent a separate degree of freedom but is indistinguishable from a motion of the WI mirror.

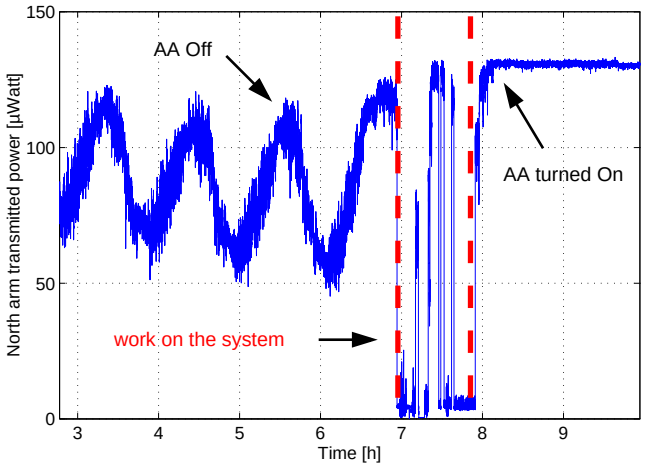

Fig. 3

LONG TERM STABILITY DUE TO THE AUTOMATIC ALIGNMENT CONTROL: THE PLOT SHOWS THE LIGHT POWER TRANSMITTED BY THE NORTH CAVITY AS A FUNCTION OF TIME. ON THE LEFT (TIME$<$ 7 H) THE AUTOMATIC ALIGNMENT (AA) WAS SWITCHED OFF, THEN AFTER A SHORT PERIOD IN WHICH THE SYSTEM WAS PREPARED FOR THE C2 RUN, THE CAVITY IS CONTROLLED AGAIN, THIS TIME WITH THE AUTOMATIC ALIGNMENT TURNED ON SO THAT THE POWER FLUCTUATIONS ARE REDUCED.

IV. EXPERIMENTAL DEMONSTRATION

The commissioning of the full VIRGO detector was started in September 2003 with the alignment of the IMC output beam through the 3 km long arms. Step by step, the interferometer length control systems have been implemented. In the meantime, the automatic alignment of the mirrors of the north arm had been implemented. In January 2004, the automatic alignment control could be started for the first time on one of the long cavities.

After the length control of the two arm cavities had been implemented, the interferometer was used in the so-called recombined configuration, in which also the position of the beam splitter is controlled so that the outgoing beams interfere destructively (output port B1). This operating condition is called *dark fringe*. It turned out that the longitudinal control is very sensitive to mis-alignments of the mirrors. A reliable lock acquisition of the recombined interferometer required the linear alignment being engaged for the arm cavities.

Approximately every two months a short period of continuous data taking, a so-called *commissioning run*, has been scheduled. The data recorded during these runs are used to monitor the progress of the commissioning of the instrument and allow to evaluate the performance of the subsystems and control systems. So far, four such runs (C1 to C4) have been performed.

During the C2 run the automatic alignment of the north arm cavity was used for the first time in a data taking period. The presence of the alignment control reduces the power fluctuations in the cavity considerably and allows long continuous operation without manual re-alignment of the optics, see Figure 3. Period of continuous operation of up to 32 hours prove the reliability of the system with the alignment control.

In the following commissioning runs the performance of the system was further improved. The alignment control systems can be used without change with one single cavity or within the recombined configuration. It allows to reduce the RMS alignment fluctuations of the mirrors can be reduced to less than 1 microradian, see Figure 4. Below the unity gain frequency (between 3 Hz and 5 Hz) the mirror motion is reduced by the control loop. For larger Fourier frequencies a slight suppression of the alignment in-loop signal can be observed because the lower RMS misalignment reduces the coupling of noise into the alignment signal.

The system has proved to be easy to use and robust: the automatic mirror alignment is now part of the standard working condition of the VIRGO interferometer. The switching of the control authority from local controls to linear alignment can be preformed without losing the longitudinal control.

The control system is designed to be limited by shot noise at a level of 10^{-13} radians$/\sqrt{\text{Hz}}$. Since the light power in the recombined configuration is about 500 times lower than in the final configuration the shot-noise limit could not yet be achieved. The sensitivity of the interferometer is currently too low to be spoiled by excess noise from the alignment control loops.

The linear alignment error signals could be used to identify resonances of the mirror suspension system which showed a larger amplitude than expected. However, in the frequency range between 100 mHz and 10 Hz the alignment error signals as shown in Figure 4 are coherent with control signal of the input mode cleaner. It is likely that the performance today is limited by the beam jitter. Further experiments are currently carried out to investigate the performance of the input beam control system.

V. Conclusion

The VIRGO interferometer has been operated for several month in the recombined configuration, in which the power-recycling cavity is not yet used. This configuration is not sensitive enough to detect gravitational waves but it allowed to implement and test the various subsystems of the detector. During this commissioning work we have successfully implemented for the first time an automatic mirror alignment system for a large-scale interferometer using the Anderson technique. At the same time this demonstrates also for the first time the automatic alignment control of a 3 km long Fabry-Perot with its mirrors suspended by complex superattenuator.

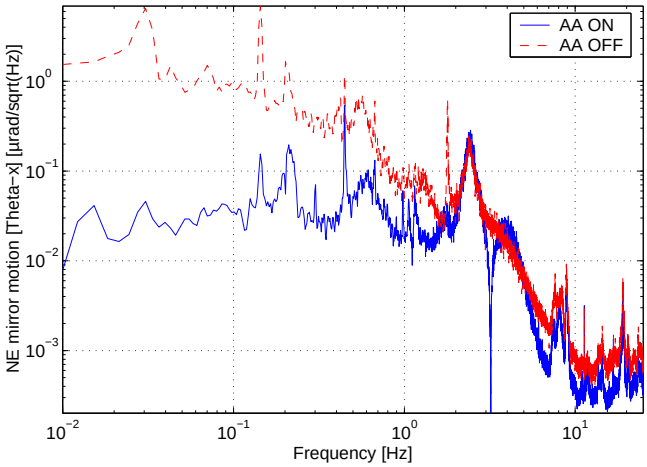

Fig. 4

Comparison of the noise spectral density of the NE mirror motion in Θ_x for automatic alignment switched on and off (measured in-loop). Below the unity gain frequency (around 3 Hz) the mirror motion is dominated by suspension resonances of the cavity mirrors or the IMC. For higher frequencies the amplitude falls rapidly to ≈ 1 nrad$/\sqrt{\text{Hz}}$ at 10 Hz. The noise floor for frequencies above 1 Hz is correlated to the laser frequency noise.

The delicate optical configuration which is necessary for the Anderson technique has been set up correctly. The switching between the local control systems of the superattenuator and the alignment control works well. A good long-term stability and noise performance of the control loops has been demonstrated. Thus the control design for the linear alignment of the full detector has been validated. Currently the implementation of the full automatic alignment system including the power-recycling mirror is under way.

References

[1] C. Bradaschia *et al.*, *Nuclear Instruments and Methods in Physics Research A* **289**, 518–525 (1990).

[2] G. Ballardin, *et al.*, "Measurement of the VIRGO superattenuator performance for seismic noise suppression", *Rev. Sci. Instrum.* **79** 9, 3643 (2001).

[3] D. Sigg *et al.*, "Commissioning of the LIGO detectors", *Class.Quant.Grav.*, **19(7)**, 1429–1435 (2002).

[4] M.Ando *et al.*, *Current status of TAMA*, *Class.Quant.Grav.* **19(7)**, 1409–1419,(2002).

[5] B. Willke *et al.*, *The GEO 600 gravitational wave detector*, *Class.Quant.Grav.*, **19(7)**, 1377–1387 (2002).

[6] F. Acernese, *et al.*, "Length sensing and control in the Virgo Gravitational Wave Interferometer", *this issue*.

[7] F. Acernese, *et al.*, "A local control system for the test masses of the Virgo gravitational wave detector", *Astrop. Phys.*, **20** (6), 617–628 (2004).

[8] D. Babusci, H. Fang, G. Giordano, G. Matone, L. Matone, V. Sannibale, “Alignment procedure for the VIRGO interferometer: experimental results from the Frascati prototype”, *Phys. Lett. A* **226**, 31–40 (1997).
[9] D. Z. Anderson, “Alignment of resonant optical cavities”, *Appl. Opt.* **23** 2944–2949 (1984).
[10] E. Morrison, B. .J. Meers, D. I. Robertson and H. Ward: “Automatic alignment of optical interferometers”, *Appl. Opt.* **33** 5041–5049 (1994).
[11] F.Cavalier, Le controle global de VIRGO, thèse d’habilitation à diriger des recherches, Université Paris Sud, LAL 01-69 (2001)
[12] F. Acernese, *et al.*, ”First locking of the Virgo central area interferometer with suspension hierarchical control”, *Astrop. Phys.*, **20** (6), 629–640 (2004).